INL/CON-14-33982
PREPRINT

Validation of the Physics Analysis used to Characterize the AGR-1 TRISO Fuel Irradiation Test

Proceedings of ICAPP 2015

James W. Sterbentz, Jason M. Harp, Paul A. Demkowicz, Grant L. Hawkes, Gray S. Chang

May 2015

The INL is a
U.S. Department of Energy
National Laboratory
operated by
Battelle Energy Alliance

Proceedings of ICAPP 2015
May 03-06, 2015 – Nice (France)
Paper 15497

Validation of the Physics Analysis used to Characterize the AGR-1 TRISO Fuel Irradiation Test

James W. Sterbentz, Jason M. Harp, Paul A. Demkowicz, Grant L. Hawkes, Gray S. Chang
Idaho National Laboratory
2525 Fremont, MS 3870, Idaho Falls, Idaho 83415
+1 (208) 526-9810 James.Sterbentz@inl.gov

Abstract – *The results of a detailed physics depletion calculation used to characterize the AGR-1 TRISO-coated particle fuel test irradiated in the Advanced Test Reactor (ATR) at the Idaho National Laboratory are compared to measured data for the purpose of validation. The particle fuel was irradiated for 13 ATR power cycles over three calendar years. The physics analysis predicts compact burnups ranging from 11.30-19.56% FIMA and cumulative neutron fast fluence from 2.21–4.39E+25 n/m^2 under simulated high-temperature gas-cooled reactor conditions in the ATR. The physics depletion calculation can provide a full characterization of all 72 irradiated TRISO-coated particle compacts during- and post-irradiation, so validation of this physics calculation was a top priority. The validation of the physics analysis was done through comparisons with available measured experimental data which included: 1) high-resolution gamma scans for compact activity and burnup, 2) mass spectrometry for compact burnup, 3) flux wires for cumulative fast fluence, and 4) mass spectrometry for individual actinide and fission product concentrations. The measured data are generally in very good agreement with the calculated results, and therefore provide an adequate validation of the physics analysis and the results used to characterize the irradiated AGR-1 TRISO fuel.*

I. INTRODUCTION

The U.S. Department of Energy in collaboration with Idaho National Laboratory and Oak Ridge National Laboratory is currently pursuing the development of high-integrity tri-structural isotropic (TRISO) coated particle nuclear fuel for next generation high-temperature gas-cooled reactor (HTGR) nuclear plants. A series of fuel tests known as the advanced gas reactor (AGR) irradiation tests are currently underway at the Idaho National Laboratory in the Advanced Test Reactor (ATR). Four AGR irradiation tests have been planned, the first three have already undergone irradiation, the fourth and final test is being designed, and the first test, AGR-1, has undergone post-irradiation examination (PIE).

The AGR-1 TRISO-coated particle test was a proof-of-process shakedown test, the first in the AGR series of tests designed to assess the fuel performance characteristics of TRISO-coated particle fuel under high temperature gas-cooled reactor irradiation conditions. The AGR-1 TRISO particle fuel was fabricated in the United States using insights gained from the study of the high-quality fuel developed under the German programs of the 1970s [1]. These insights provided the basis for the current improved U.S. TRISO particle fabrication processes.

The AGR-1 particle fuel was irradiated in the ATR over a period of three years, 13 ATR power cycles, and 620 effective full power days (EFPD) of irradiation, or 662 depletion calculation timesteps. A total of 72 fuel compacts, each containing a nominal 4,100 TRISO particles, were irradiated to varying degrees of burnup depending on vertical position in the ATR active core. Some of the TRISO-particle compacts were driven to very high burnups, accumulating substantial fast fluence, and enduring long periods of time at elevated temperatures. Throughout the AGR-1 test, there were no particle failures as assessed by careful measurement of capsule sweep gas using on-line gamma spectroscopy [2]. The AGR-1 test has now become an important benchmark test for detailed compact characterization and definition of the irradiation conditions.

In addition, a detailed physics depletion calculation for these AGR-1 conditions provided estimates of local neutron flux, neutron spectra, nuclear reaction rates, fission and radiation energy deposition rates, as well as fission product and actinide concentrations for every compact and capsule at each timestep from beginning-of-irradiation (BOI) to end-of-irradiation (EOI). Some of these calculated physics data became input data for other analyses: heat rates and fast fluence for the thermal analysis, gaseous

radionuclide birth rates for the release-to-birth (R/B) analysis, compact burnup for fuel performance model analysis, calculated activities for source term definition, and others. Consequently, validation of the physics models, methodology, assumptions, and calculated results was important to establish confidence in the calculated physics data and to understand the overall performance of the AGR-1 TRISO-particle fuel.

Validation of the physics calculation was done by comparing the calculated results with corresponding PIE measurement data from the AGR-1 test using a variety of measurement techniques: 1) high-resolution compact gamma spectroscopy (gamma scans) for detailed axial burnup and isotopic activity estimates for all 72 compacts, 2) inductively coupled plasma mass spectrometry (ICP-MS) for compact burnup as well as actinide and fission product masses using four selected compacts, and 3) flux wire activities for fast neutron cumulative fluence. The mass spectrometry measurements were limited to four AGR-1 compacts that spanned the calculated burnup range. Only four compacts underwent PIE because of the multi-step, time-intensive processing of radioactively-hot compacts. These four compacts were de-consolidated. Individual particles were randomly selected in batches of 20 fuel kernels, the kernels were dissolved, and the solutions were analyzed using ICP-MS [3].

Comparison of the AGR-1 measured data with the corresponding calculated physics data shown later in this paper produced generally good to excellent agreement. This agreement forms the basis for the validation of the detailed physics depletion calculation and its resulting compact characterization data.

II. TRISO PARTICLES

Specific mean-value characteristics of the AGR-1 baseline TRISO particles are given in Table I [4]. These values were used in the physics depletion calculations. The uranium oxy-carbide kernel (UCO) microsphere had a nominal diameter of 350 μm and an enrichment of 19.74 wt% U235.

TABLE I

AGR-1 TRISO particle as-built characteristics.

Property	Baseline
UCO kernel diameter (μm)	349.7 ± 9.0
UCO kernel density (g/cm^3)	10.924 ± 0.015
U-235 enrichment (wt%)	19.736 ± 0.047
C/U Atom Ratio	0.3253 ± 0.0028
O/U Atom Ratio	1.3613 ± 0.0064
Buffer thickness (μm)	103.5 ± 8.2
Buffer density (g/cm^3)	1.10 ± 0.04
IPyC thickness (μm)	39.4 ± 2.3
IPyC density (g/cm^3)	1.904 ± 0.014
SiC thickness (μm)	35.3 ± 1.3
SiC density (g/cm^3)	3.208 ± 0.003
OPyC thickness (μm)	41.0 ± 2.1
OPyC density (g/cm^3)	1.907 ± 0.008
Particle diameter (μm)	799.7
U (g/compact)	0.917
Particles per compact	4154
Particle packing fraction	36.0 to 37.4%

III. FUEL COMPACTS

The TRISO particles were bound together with a graphite matrix material and formed into cylindrical fuel compacts. Each compact had a diameter of approximately 1.23 cm, length of 2.51 cm, and contained 4154 particles. The graphite binder matrix had an average density of 1.3 g/cm^3. The AGR-1 baseline compacts nominally contained 0.1810 g U235 and 0.7329 g U238.

Figure 1 is a radiograph of an AGR-1 fuel compact. The dark grey dots are the high density UCO kernels. The light grey background is the lower density graphite matrix and particle coatings. The kernel density appears to decrease from center to periphery due to the increased thickness traversed by the x-rays at the center of the cylindrical compact relative to the outer edges.

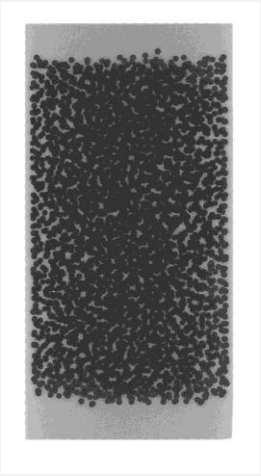

Figure 1. Radiograph of an AGR-1 fuel compact.

The AGR-1 compacts also had special top and bottom graphite end caps for particle protection during sintering (Figure 1). The endcaps were made from the same material as the graphite binder matrix and ranged in thickness from 1-2 mm. The average compact packing fraction was approximately 37%. The particle packing fraction in the fueled middle region of the compacts was estimated to be approximately 40-41%; the physics model used 40.8% with top and bottom endcap thicknesses of 2.0 and 1.6 mm, respectively.

IV. AGR-1 CAPSULE DESIGN

The AGR-1 experiment was composed of six vertically-stacked capsules, all part of an instrumented test

train [4, 5] designed to fit into the 3.81 cm diameter B-10 test facility in the ATR beryllium reflector (Figure 2). Each capsule is approximately 3.49 cm in diameter and 15.24 cm in length (Figures 3 and 4). The capsules are stacked vertically one atop the other with capsule 1 at the bottom and capsule 6 at the top. The core midplane is between capsules 3 and 4; the maximum ATR neutron flux intensity

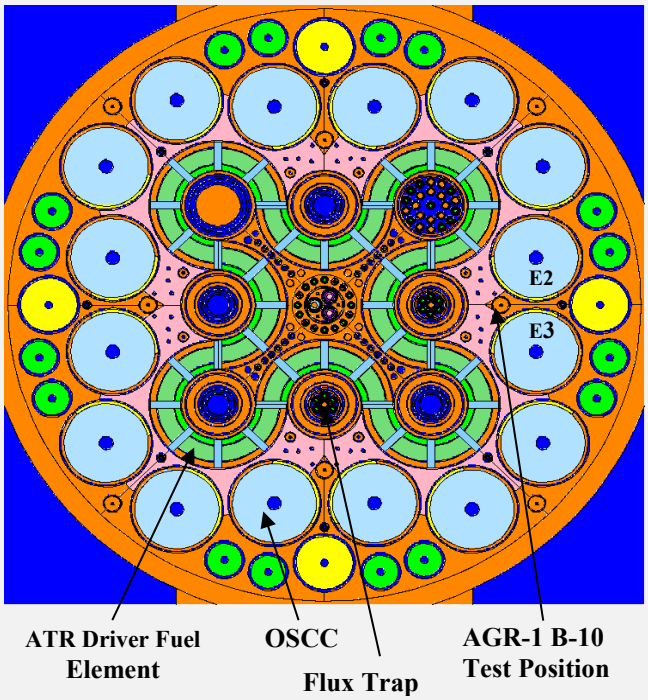

Figure 2. Cross section view of the ATR core.

occurs just below the midplane. Figure 5 shows an axial cross section view of the six capsules and two of the three compact stacks with each compact subdivided into two axial pieces.

In each of the six AGR-1 capsules, there were 3 parallel stacks of compacts with 4 compacts per stack for a total of 72 compacts. Individual compacts are designated by capsule, level, and stack. For example, 3-2-1 refers to the compact in capsule 3, level 2, stack 1. Level refers to the 4 vertically-stacked compacts with level 1 at the bottom of the stack and level 4 at the top.

Borated graphite holders support the 3 compact stacks in each capsule. The holder is a solid cylindrical piece of nuclear-grade graphite with three holes drilled axially, one for each compact stack. Natural boron carbide (B_4C) is uniformly dispersed throughout the graphite holder as a burnable poison to limit the beginning-of-irradiation (BOI) compact fission rate. The four middle capsules contained approximately 7.0 wt% B_4C and the two end capsules 5.5 wt%. The boron-10 burned out after the 6th ATR cycle. The graphite holders also contained embedded flux monitors, gas lines, thermocouples (TC), and thru-tubes containing gas lines as well as TCs for the capsules below. The graphite holder along with the inner capsule wall formed temperature-controlling gas gaps.

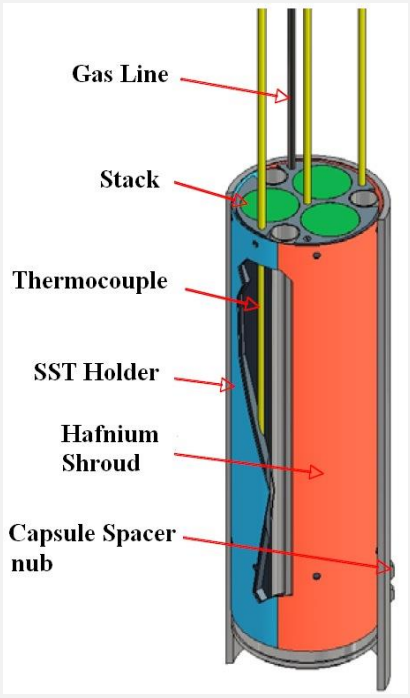

Figure 3. Cutaway view of a single AGR-1 capsule.

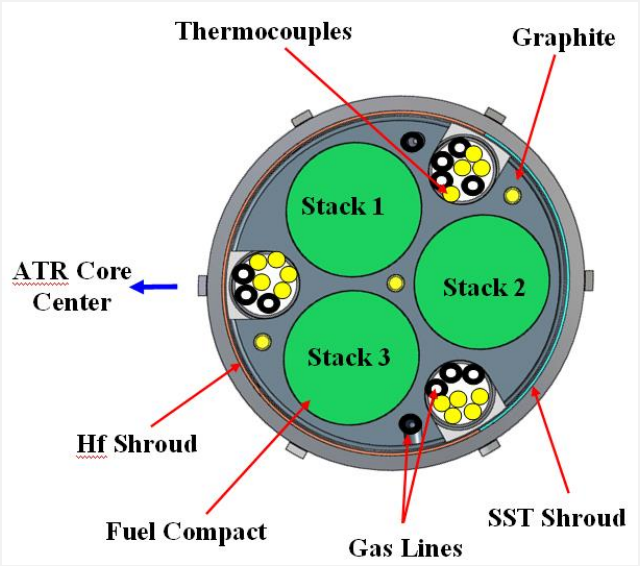

Figure 4. Cross section view of a typical AGR-1 capsule.

The temperature of each capsule was independently controlled with the gas gaps by means of a variable neon-to-helium gas mixture ratio. The gap thicknesses were determined prior to irradiation. The mixture ratio was adjusted during irradiation using a designated TC. The slow-flowing helium/neon gas also collected radioactive fission gases released from the TRISO-particle compacts

which were counted downstream using the fission product gas monitoring system. The fission gas monitoring system provided a means to detect particle failures during irradiation and also estimate gaseous fission product release rates.

Outside each of the stainless steel (SST) capsules was a cylindrical neutron filter (shroud). The shroud was constructed of three concentric tubes. The inner and outermost tubes were made of stainless steel and the middle tube was a 240° sector of natural hafnium metal and a 120° sector of stainless steel. The hafnium sector faced the ATR core center to reduce the strong thermal flux coming from the direction of the ATR driver core. The hafnium transmuted slowly over the 13 ATR cycles and helped maintain a more uniform fission rate in all three compact stacks in each capsule over the entire 13-cycle irradiation.

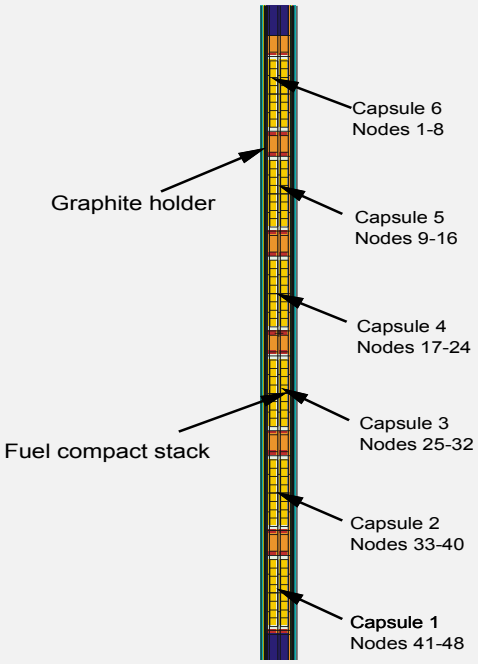

Figure 5. Axial cross section view of the six capsules showing two of the three compact stacks in each capsule and 2 calculation nodes or cells per compact.

V. ADVANCED TEST REACTOR

The Advanced Test Reactor (ATR) is a thermal reactor with an active core of high-enriched, light water-cooled, aluminum plate fuel elements. The driver core is composed of 40 fuel elements arranged in a distinctive serpentine or cloverleaf configuration creating a 3x3 array of cylindrical flux traps (Figure 2). The active core is moderated and reflected with a beryllium reflector; the beryllium reflector contains 16 outer shim control cylinders (OSCC) and 75 test facilities for experiments. The ATR core is rated at 250 MW, but currently operates nominally around 110 MW.

The AGR-1 experiment was located in the B-10 test facility which is radially out beyond the outboard east flux trap and sandwiched between the E2 and E3 OSCCs (Figure 2). Hafnium plates attached to the rotatable OSCCs were used to adjust the five inboard lobes that make up the serpentine active core. The AGR-1 test train was then situated very close to the E2 and E3 OSCCs which impacted the compact fission power as a function of OSCC rotation. The greatest impact occurs typically at the end of each cycle when the OSCCs are rotated to extreme angles and fission rates can increase significantly (up to 30%) relative to beginning-of-cycle.

VI. DEPLETION METHODOLOGY

The AGR-1 physics depletion calculation was a detailed Monte Carlo depletion calculation that used the MCNP [6] and ORIGEN2.2 [7] computer codes linked with the JMOCUP utility program [8, 9]. NJOY [10] was used to generate ENDF-7 temperature-dependent neutron cross sections for the fuel (600 and 1200 ºC). A detailed description of the AGR-1 physics calculation is given in reference [11].

The MCNP code was chosen because of its ability to model three-dimensional and highly heterogeneous geometric structures, such as the ATR core and the AGR-1 experiment. In addition, MCNP provides an exact Monte Carlo solution to the transport equation, continuous energy cross sections, and has the ability to calculate neutron, gamma, and beta energy deposition rates. The MCNP model used in this analysis includes the entire 40-element ATR driver core, 9 flux traps plus experiments, 16 beryllium blocks, multiple beryllium facility experiments including the AGR-1 test in the B-10 position, 16 outer shim control cylinders, neck shim housing, 24 neck shim rods, hafnium safety rods, supporting reactor structures, thermal shields, and pressure vessel structures. The AGR-1 MCNP models have undergone independent technical review checks as part of the verification process for the physics depletion calculation [11].

This physics depletion calculation was composed of four separate depletion calculations: 1) 40 ATR driver fuel elements, 2) AGR-1 compacts, 3) AGR-1 hafnium shroud, and 4) AGR-1 borated graphite holders. The 13 ATR irradiation cycles were subdivided into 662 depletion timesteps or approximately one timestep per 24-hour period over the 620 effective full power days included in this study. At each timestep, in addition to the four depletions, the OSCCs rotated, and neck shim rods were removed from the core according to the as-run ATR power and control element measured data. In this manner, the simulated ATR mimicked the criticality of the actual ATR core. The physics calculation maintained a k-effective very near 1.0 during each ATR power cycle. As an example, Figure 6 shows the calculated ATR core k-effective as a function of timestep for cycle 145A. Cycle 145A is typical

of the other 12 AGR-1 cycles and shows the k-effective close to 1.0 over the entire cycle. It is interesting to note there were 3 scrams during this cycle as evidenced by the three downward spikes in the curve. The upward spikes correspond to neck shim rod removals during a particular timestep. The calculated k-effective curves for each cycle demonstrated that the physics depletion calculation computed properly and provided verification that the computer codes, models, ATR input data, and modeling assumptions were reasonable.

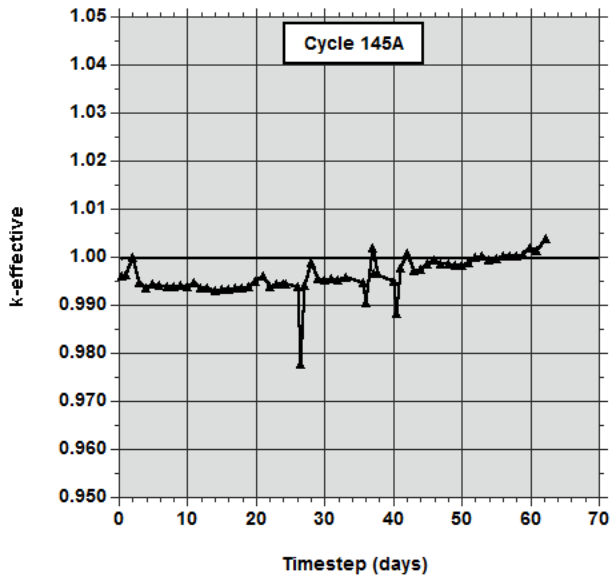

Figure 6. Typical calculated k-effective versus timestep.

Two distinct MCNP models were constructed for the AGR-1 physics depletion analysis, one with the compacts homogenized and the other with the individual TRISO-particles explicitly modeled with all coatings. Both models were used to calculate compact heat rates, neutron flux, fast fluence, nuclear reaction rates, nuclide inventories, and burnup. The more accurate model is the particle model and all results reported here are from the particle model except where explicitly noted. The particle model produced more accurate EOI nuclide inventories, especially for the plutonium isotopes. The homogenized compact model was used primarily for comparative purposes.

A cross section view of a compact in the particle model using a regular array of particles is shown in Figure 7. There are 173 TRISO particles per layer of particles and 24 particle layers per compact for a total of 4152 particles per compact. Although difficult to see in the figure, the kernel, buffer, and inner pyrolytic carbon, silicon carbide, and outer pyrolytic carbon coatings are explicitly modeled. The compacts were subdivided into two equal axial volumes each containing 12 particle layers or 2076 particles. This compact subdivision added resolution to the calculated axial heat rates and burnups.

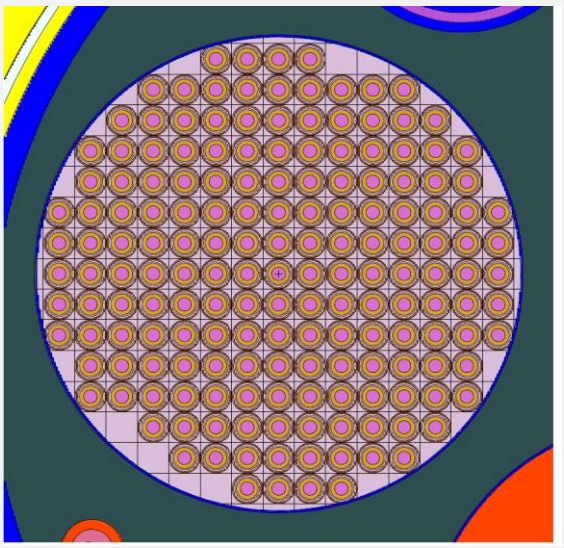

Figure 7. Particle model cross section view of TRISO particles in a compact.

VII. RESULTS

This section discusses and compares the calculated and measured compact burnup, fast fluence, and nuclide inventory results.

VII.A. Burnup

The AGR-1 compacts sustained significant burnups over the 13 cycle exposure in ATR with calculated end-of-irradiation burnups ranging from 11.30-19.56% FIMA (fissions of initial heavy metal atoms). Table II lists the individual calculated compact average burnup by capsule, level, and stack. These percent values indicate that approximately 11-20% of the initial uranium inventory in each compact has been fissioned with the bulk of the fissions attributed to U235. For compact 3-4-3 (maximum burnup compact), approximately 78.6% of the total fissions are from U235, 17.6% from Pu239, 3.6% from Pu241, and 0.3% from U238.

TABLE II

Calculated EOI compact burnups (% FIMA).

Capsule	Level	Stack 1	Stack 2	Stack 3
6	4	13.35	11.30	13.35
6	3	13.53	11.43*	13.58
6	2	14.20	12.05	14.17
6	1	15.25	12.79	15.28
5	4	16.99	14.25	17.01
5	3	16.93*	14.18	17.01
5	2	17.37	14.64	17.42
5	1	18.22	15.82	18.19
4	4	18.96	16.74	18.99
4	3	18.60	16.38	18.63
4	2	18.81	16.64	18.83

4	1	19.38	17.39	19.43
3	4	19.48	17.56	19.56
3	3	19.07	17.02	19.17
3	2	19.07*	17.02	19.12
3	1	19.50	17.58	19.53
2	4	19.09	17.14	19.12
2	3	18.39	16.33	18.49
2	2	18.18	15.97	18.26
2	1	18.39	16.28	18.49
1	4	17.28	14.93	17.36
1	3	16.14*	13.82	16.30
1	2	15.45	13.35	15.60
1	1	15.19	13.22	15.32

** ICP-MS analysis was performed on these 4 compacts.*

Stack 2 burnup is consistently less than stacks 1 and 3 by approximately 10-15%, because stack 2 was farther from the core center, shadowed by stacks 1 and 3, and was in closer proximity to the thermal neutron absorbing hafnium plates on the E2 and E3 OSCCs. Hence, the thermal neutron flux at the compact stack 2 location was always slightly less relative to stacks 1 and 3.

The higher burnups of stacks 1 and 3 are notably almost identical due to symmetry considerations. Only slight burnup differences in these two stacks result from small rotational differences in the two OSCCs and differences in the ATR driver fuel element loadings in the serpentine portion facing the B-10 test facility.

A substantial effort was invested in the measurement of compact fission product activity and burnup estimation. Reference [3] gives a detailed description of the gamma spectrometry using the INL Hot Fuel Examination Facility (HFEF) precision gamma scanner (PGS) and the two affiliated methods (direct and ratio) used to estimate compact average burnups in %FIMA. Plus, inductively coupled plasma mass spectrometry (ICP-MS) measurements were used on a limited number of compacts to confirm the PGS burnups and produce both EOI actinide and fission product nuclide inventories. Table III summarizes the measured burnup estimates.

TABLE III

Compact burnup comparison (% FIMA).

Compact	Particle Model	PGS Direct	PGS Ratio	ICP-MS
6-3-2	11.43	10.7	11.0	10.7
5-3-1	16.93	16.9	15.9	16.3
3-2-1	19.07	18.2	18.6	19.3
1-3-1	16.14	16.0	15.6	16.3

The PGS direct method used measured Cs137 activities to estimate burnup. The test-average (all 72 compacts) calculated-to-experimental ratio, or C/E ratio, for the Cs137 activity was 1.0013±0.0319 and for Cs134 was 1.0190±0.0506 for all compacts [3]. This result provides solid validation for the calculation, since Cs137 is the optimal direct burnup indicator. The PGS direct method burnups rely on the initial fissile inventory at each gamma scan slice of a compact and because of the random distribution of particles axially in each compact, this leads to some uncertainty in the axial burnup of the compacts.

The PGS ratio method however does not rely on the initial fissile inventory and is believed to be more accurate. The ratio method uses the activity ratio of Cs134/Cs137 to determine burnup. Figure 8 compares the ratio method burnups with the calculated burnups as a function of compact axial position. The measured burnups are color-coded by capsule with the calculated values overlaid (yellow diamonds). The calculation gives an axial resolution of two points per compact (average value for the two axial halves of each compact), whereas the measurement provides a high-resolution distribution, or approximately 9 axial points per compact.

In Figure 8, the lower of the three curves for each capsule is always stack 2 with a smaller burnup relative to stack 1 and 3 compacts, as discussed previously. The measured burnups between the two high burnup stacks 1 and 3 shows some noticeable difference in contrast to the calculated values for these two stacks which are nearly identical. This differentiation in the measured values appears to increase from capsule 6 (top-of-core) to capsule 2. The calculation does not exhibit this difference despite the careful inclusion of each OSCC bank rotation by timestep and modeling of the BOL ATR fuel element loading. However, upon more careful inspection, capsule 1 does show a slight visible difference between stacks 1 and 3 calculated burnups. The higher stack 3 burnup is attributed to the standard core flux tilt and slight variations in the outer shim control cylinder rotations on either side of the AGR-1 irradiation position in the ATR beryllium reflector.

An interesting feature in both calculated and measured burnups is the peaking at both ends of each capsule. The finer axial burnup resolution of the measurement shows a much more pronounced peaking than the calculation. The peaking is real and attributed to thermal neutron in-leakage into the top and bottom of each capsule due to the fact that the borated graphite holders do not extend beyond the top of the top compact (level 4) nor below the bottom of the bottom compact (level 1). Had the borated graphite holder been extended at each end or borated graphite endcaps placed on both ends of the holder, the peaking would have been reduced. It could be surmised that the actual maximum measured peak particle burnup is approximately 21.0% FIMA (compacts 3-1-1 and 3-1-3) or possibly slightly greater considering the measurement uncertainty.

A second measurement technique was employed, namely ICP-MS, to estimate compact burnup as a verification of the PGS burnup measurements. Table III compares the PGS and ICP-MS measured burnups to the calculated particle model burnups for the four AGR-1 compacts that underwent ICP-MS burnup analysis.

The ICP-MS burnup measurements are in very good agreement with PGS burnup estimates and the calculated burnups (±3-7%). Although not shown in Table III, the minimum burnups occur in compact 6-4-2 in all cases; the maximum in capsule 3, stack 3, all just below core midplane, as expected.

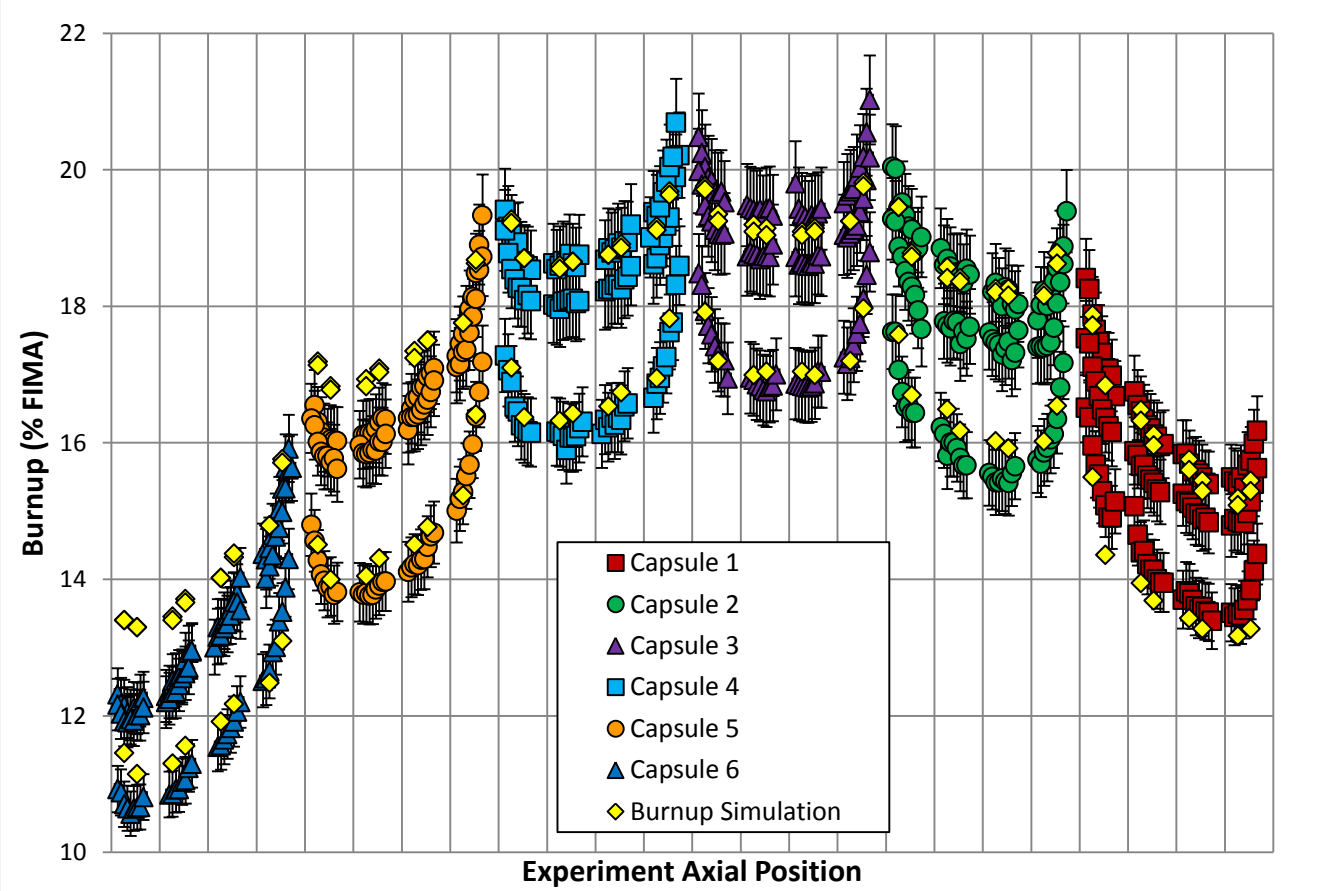

Figure 8. Axial compact burnup estimates (%FIMA) using the PGS ratio method versus burnup simulation (calculation).

VII.B. Nuclide Activities and Concentrations

Actinide and fission product nuclide activities and concentrations were calculated at each timestep for all 72 compacts. As an example, Figure 9 shows the specific uranium and plutonium isotopic mass concentrations in units of grams per initial gram of uranium metal in the compact as a function of burnup (GWD/MTU, gigawatt-days per metric ton of initial uranium) for the maximum burnup compact 3-4-3 (19.56% FIMA).

Compact 3-4-3 had an initial uranium mass of 0.9170 g U, 0.0028 g U234, 0.1810 g U235, 0.0003 g U236, and 0.7329 g U238. By EOI, this compact had a calculated U235 mass of only 0.0145 grams (92% depletion) or a burnup of ~190 GWD/MTU. The plutonium isotopic concentrations increased during the irradiation as shown in Figure 9. Near EOI, both the Pu239 and Pu240 concentrations begin to decrease as the compact is driven by the ATR driver core flux.

Calculated EOI nuclide inventories were compared against PGS measured activities and ICP-MS measured nuclide concentrations for the four compacts that underwent destructive examination. Table IV gives test-

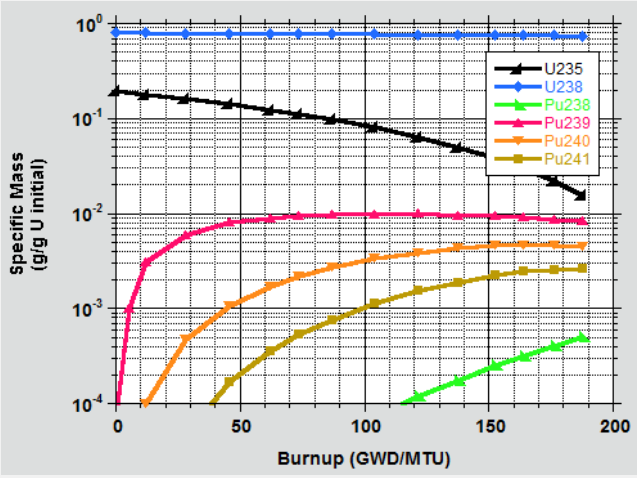

Figure 9. Compact 3-4-3 uranium and plutonium isotopic specific mass versus burnup (GWD/MTU).

average calculated-to-experimental (C/E) activity ratios for important burnup fission products [3] based on gamma spectrometry of whole compacts. Test-average means the average over all the 72 compacts.

TABLE IV

C/E activity ratios for some fission products.

Isotope	C/E	Uncertainty	Type
Cs137	1.0013	±0.0319	direct
Cs134	1.0190	±0.0506	shielded
Ce144/Pr144	0.9939	±0.0367	direct
Ru106	1.0404	±0.0432	direct
Eu154	1.1835	±0.0525	shielded
Sb125	1.3955	±0.0860	direct

Table V gives uranium, plutonium, and selected fission product C/E concentration ratios for three samples examined from compact 3-2-1 (based on ICP-MS measurements). Each sample consisted of 20 randomly selected TRISO fuel particles collected from the compact after electrolytic deconsolidation [12]. The relative uncertainty for the ICP-MS measurements is 5%. Compact 3-2-1 is the high burnup compact (19.07% FIMA) of the four compacts that underwent ICP-MS burnup analysis.

TABLE V

C/E concentration ratios for compact 3-2-1.

Isotope	Sample 1	Sample 2	Sample 3
U234	0.99	1.07	1.02
U235	0.96	0.98	0.99
U236	1.05	1.12	1.07
U238	1.05	1.12	1.08
Pu239	1.33	1.31	1.22
Pu240	1.32	1.30	1.16
Pu241	1.25	1.25	1.15
Pu242	1.25	1.27	1.16
La139	0.92	0.99	0.94
Ce140	1.25	1.32	1.24
Pr141	0.87	0.93	0.89
Ce142	1.26	1.34	1.25
Nd145	0.87	0.93	0.88
Nd146	1.04	1.12	1.07

The C/E activity ratios for Cs137, Cs134, Ce144/Pr144, and Ru106 in Table IV are within a few percent of 1.0 which means the calculated values are in excellent agreement with the measured values. Cs134 is a shielded fission product which is more difficult than a direct fission product to calculate accurately. Eu154 and Sb125 are in reasonable agreement but are high by 18-40% which would indicate a slight measurement or calculational bias. Direct fission products are produced directly from fission or a subsequent beta decay chain, while shielded fission products are produced by the neutron capture of a direct fission product and have a stable nuclide of the same atomic mass that prevents or shields production from beta decay from lower atomic mass nuclides. For example, Xe134 (direct) is stable ending the A=134 beta decay chain, whereas Cs134 (shielded) is produced from the neutron capture of Cs133 (direct).

The C/E ratios for the uranium isotopes and some of the fission products in Table V are close to 1.0. This is especially true for U235 which is within a few percent for all three samples. The plutonium C/E ratios were high by approximately 15-30%. Possible reasons include: 1) the calculation over-predicts the plutonium concentrations or 2) sample dissolution did not recover all of the plutonium from the kernels. It is not clear at this point which one, or if both of these possible issues are responsible for the high plutonium C/E ratios. The calculated values used for Table V are from the particle model, values from the homogenized compact model were even higher.

Although the C/E values for plutonium are high by 15-30%, the difference has little impact on the burnup evaluation (as seen in Table III) given the initial U235 enrichment (19.7%) and burnups up to 20% FIMA. Plutonium only accounts for about 4% of the end of irradiation actinide mass for the highest burnup compacts and less in the lower burnup compacts.

The various iterations in sample preparation and several iterations modifying the simulations were unable to resolve the discrepancies between recovered plutonium and the expected inventory, nor positively identify if the bias was in the experimental measurements, the simulations, or both. Due to the challenges inherent in the handling and processing of irradiated coated particles, the precise mass of the 20 kernels analyzed in each case was not known prior to dissolution. Variations in the as-fabricated AGR-1 kernel size (kernel mean diameter was 350 μm with a standard deviation of 9.0 μm) could bias the comparison of predicted actinide inventory with the measured values. However, the mass of fuel leached is not required for the burnup evaluation as burnup is calculated from only the relative amounts of material in each mass spectrometry sample.

The initial physics depletion calculation used a homogenized compact model in which the TRISO particle number densities were smeared over the compact volume. The homogenized model produced C/E ratios for the plutonium isotopic concentrations that were 20-50% high. It was speculated that the homogenization reduced the self-shielding of the U238 atoms and enhanced the U238 radiative capture and higher plutonium transmutation rates. This led to the development of the particle model in which the UCO kernels were explicitly modeled as spheres (lumped fuel). The particle model provided enhanced self-shielding of the U238 atoms and a subsequent reduction in the plutonium isotopic concentrations. Table VI compares the C/E ratios for the two models using the 3 measured samples for compact 3-2-1. These results clearly demonstrate the need to explicitly model the individual

TRISO particles in each compact in order to get higher-order actinide inventories as accurate as possible.

TABLE VI

C/E ratios for particle versus homogenized models.

Model	Pu239	Pu240	Pu241	Pu242
Particle	1.33	1.32	1.25	1.25
Particle	1.31	1.30	1.25	1.27
Particle	1.22	1.16	1.15	1.16
Homog.	1.54	1.51	1.45	1.31
Homog.	1.52	1.49	1.45	1.34
Homog.	1.41	1.34	1.33	1.22

VII.C. Fast Neutron Fluence

The neutron energy flux was calculated in each compact at every timestep over the 13 ATR irradiation cycles. Of particular interest was the fast neutron spectrum above 0.18 MeV (E_n>0.18 MeV). These high energy neutrons produce atomic displacement or lattice damage in all materials including the graphite holders and graphite and silicon carbide coatings in the TRISO particles. Lattice damage can change thermal conductivity and dimensions.

In order to estimate the fast fluence, the calculated energy-dependent neutron fluxes were timestep-weighted and cumulatively summed over the entire 13-cycle AGR-1 irradiation. Table VII gives the calculated total cumulative fast fluence (E_n>0.18 MeV) by compact at end-of-irradiation. The AGR-1 test requirements specified that the compact fast fluence should not exceed 5.0E+25 n/m^2 (E_n>0.18 MeV). This requirement was met with the highest total fluence reaching 4.39E+25 n/m^2 in compact 3-3-3.

TABLE VII

Calculated fast fluence (10^{25} n/m^2) by compact.

Capsule	Level	Stack 1	Stack 2	Stack 3
6	4	2.49	2.21	2.49
6	3	2.74	2.43	2.75
6	2	2.93	2.60	2.94
6	1	3.07	2.74	3.08
5	4	3.53	3.16	3.55
5	3	3.71	3.31	3.73
5	2	3.83	3.42	3.85
5	1	3.89	3.48	3.91
4	4	4.12	3.69	4.15
4	3	4.24	3.79	4.26
4	2	4.28	3.84	4.32
4	1	4.27	3.83	4.30
3	4	4.31	3.87	4.34
3	3	4.36	3.90	4.39
3	2	4.34	3.89	4.38
3	1	4.25	3.82	4.29
2	4	4.09	3.68	4.12
2	3	4.06	3.64	4.09
2	2	3.96	3.56	4.00
2	1	3.80	3.42	3.83
1	4	3.40	3.06	3.43
1	3	3.28	2.94	3.31
1	2	3.10	2.78	3.13
1	1	2.86	2.56	2.88

In order to validate the calculated EOI compact fast fluences, a comparison was made with measured data [13]. Fluence monitors were installed in the AGR-1 capsules. There were 3 monitors per capsule embedded in different locations in the graphite holders. The fluence monitors consisted of a vanadium tube measuring 0.127 cm diameter and approximately 0.762 cm long with a single small wire sealed inside. The 3 types of wires used were made of high purity: (1) iron (Fe), (2) niobium Nb, and (3) 1% cobalt-vanadium (Co-V) alloy. Each wire was typically 0.051 cm in diameter and 0.102 cm long. Each capsule contained one of each type of fluence monitor for a total of 18 fluence monitors in the AGR-1 experiment.

Following the AGR-1 irradiation, the graphite holders were crushed and the fluence monitors were retrieved. Unfortunately, the monitors from capsule 1 were not found, nor were the Co-V monitors from capsules 3 and 5. The retrieved fluence monitors in capsules 2-6 were gamma counted. The Nb wires were dissolved and x-ray counted. For the fast fluence measurements, two threshold particle reactions were used: ^{54}Fe(n,p)^{54}Mn and ^{93}Nb(n,n′)^{93m}Nb. Table VIII and Figure 10 compare the fast fluence estimates (E_n>0.18 MeV) derived from flux wire measurements and the calculated cumulative fast fluence at the flux wire locations in the graphite holders.

TABLE VIII

Fast fluence comparison (10^{25} n/m^2).

Capsule	Measured	Calculated	Δ
6	2.33 ± 7%	2.42	+3.7%
5	3.06 ± 7%	3.05	-0.3%
4	3.25 ± 7%	3.43	+5.2%
3	3.33 ± 7%	3.39	+1.8%
2	3.19 ± 7%	2.99	-6.7%
1	--	2.29	--

*Δ = [(Calculation-Measurement)/Calculation] * 100*

The uncertainty associated with the calculated values has not been estimated, but the combined errors associated with the ATR input data, number densities, statistical errors from the Monte Carlo method, etc. would be similar to the experimental error values. The agreement between measured and calculated fast fluence is very good and provides validation of both the calculated fast fluence and the calculation in general.

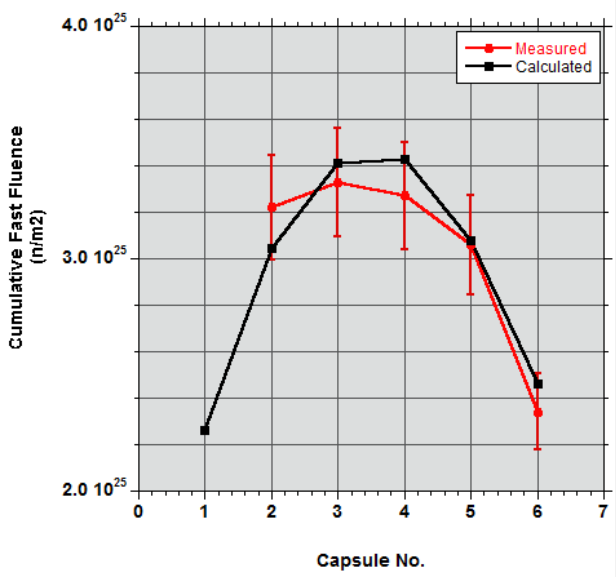

Figure 10. Fast fluence comparison between measured and calculated.

VII.D. Thermocouple Measurements

The AGR-1 test was monitored with a total of 17 thermocouples in the six capsules embedded in the graphite holders. The TCs gave a direct temperature measurement for specific locations in the graphite holder near the much hotter TRISO-particle compacts.

Six finite-element heat transfer capsule models were developed for the thermal analysis [14]. The models were used to calculate and track the daily–average TC temperature measurements over the 662 timesteps, thus providing time-dependent temperature profiles throughout the AGR-1 irradiation. Part of the thermal model input data included the physics-calculated volumetric heat rates and fast fluence for all capsule components and TRISO-particle compacts.

Because the physics-calculated heat rates and fast fluence were only part of the thermal model input, a direct validation feedback from the thermal model TC predictions and the TC measurements was not possible. However, the thermal model did give reasonable agreement with the TC readings which provided indirect feedback that the physics calculated heat rates were also reasonable.

VIII. CONCLUSIONS

The AGR-1 test was a very successful irradiation of the new US designed and fabricated TRISO-particle fuel. Despite high levels of burnups, fast neutron fluence, and long high-temperature irradiation conditions in the Advanced Test Reactor, there were no particle failures.

Characterization of the 72 TRISO-particle compacts was done with a detailed Monte Carlo physics depletion calculation which supplied estimates of compact burnup and fast fluence, as well as fission product and actinide concentrations at each of the 662 timesteps over the three year irradiation. These physics calculated results were compared against measured data in order to provide a validation basis for the calculation. Measurements supporting the validation basis included: gamma spectrometry and mass spectrometry for compact burnup (%FIMA) and isotopic activities, flux wire activation for fast fluence, and mass spectrometry for nuclide inventory.

Overall, there was very good agreement between the measurements and the calculation. Measured activities of the optimal burnup isotopes (Cs137 and Cs134) produced a calculated-to-experimental (C/E) value near 1.0. Compact-average burnups using three different measurement techniques all agreed to within ±3–7% with the calculated values over the entire AGR-1 burnup range. The high-resolution measured burnups from the PGS ratio method overlaid the calculated burnups very well. Plus, the measured and calculated burnups exhibited similar compact peaking at the top and bottom of each capsule and identified the same low burnup compact (6-4-2) as well as the highest burnup compacts in capsule 3. C/E activity ratios for four important fission products were within a few percent of 1.0, although two were biased high. The ICP-MS uranium isotopic concentration C/E ratios were in very good agreement, especially the U235 concentrations. The plutonium isotopic C/E concentration ratios were, however, slightly high by approximately 15-30%. The cumulative fast fluence (E_n>0.18 MeV) agrees to better than ±7% for all capsules.

The agreement between the AGR-1 measured data and the corresponding calculated data provides a strong and reasonable validation basis for the detailed physics depletion calculation along with the associated physics models, methodology, modelling assumptions, and the calculated results.

ACKNOWLEDGMENT

This work was supported by the U.S. Department of Energy, Next Generation Nuclear Plant Program, on the Idaho Operations Office Contract DE-AC07-05ID14517.

REFERENCES

1. D. A. PETTI, et. al., “Key Differences in the Fabrication, Irradiation, and High Temperature Accident Testing of U.S. and German TRISO-coated Particle Fuel and Their Implications on Fuel Performance,” *Nuclear Engineering and Design*, **222**, 281-297 (2003).
2. M. A. POPE, “AGR-1 Irradiation Test Final As-Run Report,” INL/EXT-10-18097, Idaho National Laboratory, Idaho Falls, Idaho, USA (2010).

3. J. M. HARP, et. al., "An analysis of nuclear fuel burnup in the AGR-1 TRISO fuel experiment using gamma spectroscopy, mass spectroscopy, and computational simulation techniques," *Nuclear Engineering and Design,* **278**, 395-405 (2014).
4. J. T. MAKI, "AGR-1 Irradiation Experiment Test Plan," INL/EXT-05-00593, Rev. 3, Idaho National Laboratory, Idaho Falls, Idaho, USA (2009).
5. S. B. GROVER, et. al., "Completion of the First NGNP Advanced Gas Reactor Fuel Irradiation Experiment, AGR-1, in the Advanced Test Reactor," *Proc. HTR-2010*, Prague, Czech Republic (2010).
6. "MCNP—A General Monte Carlo N-Particle Transport Code, Version 5/1.60," X-5 Monte Carlo Team, LA-UR-03-1987, Los Alamos National Laboratory, Los Alamos, New Mexico, USA (2008).
7. S. B. LUDWIG and A. G. Croft, "*ORIGEN2.2 – Isotope Generation and Depletion Code Matrix Exponential Method*," Oak Ridge National Laboratory, Oak Ridge, Tennessee, USA (2002).
8. R. S. BABCOCK, et. al., "The MOCUP Interface: A Coupled Monte Carlo/Depletion System," *Proc. of the Topical Meeting on Advances in Reactor Physics*, Vol. III, American Nuclear Society, Knoxville, Tennessee, USA (1994).
9. J. W. STERBENTZ, et. al., "Monte Carlo Depletion Calculation for the AGR-1 TRISO Particle Irradiation Test," *Trans. of the American Nuclear Society*, Vol. 102, San Diego, California, USA, (2010).
10. R. E. MACFARLANE, et. al., *"NJOY99.0: A Code System for Producing Pointwise and Multigroup Neutron and Photon Cross Sections from ENDF/B Data*," Los Alamos National Laboratory distributed by Oak Ridge National Laboratory Radiation Safety Information Computational Center, Oak Ridge, Tennessee, USA (1999).
11. J. W. STERBENTZ, "JMOCUP As-Run Daily Depletion Calculation for the AGR-1 Experiment in ATR B-10 Position," ECAR-958, Rev. 2, Idaho National Laboratory, Idaho Falls, USA (2013).
12. P. A. DEMKOWICZ, et. al., "Preliminary Results of Post-Irradiation Examination of the AGR-1 TRISO Fuel Compacts," *Proc. HTR-2012*, Tokyo, Japan (2012).
13. L. R. GREENWOOD, "Analysis of AGR-1 Neutron Fluence and Melt Wire Capsules," PNNL Project Number: 58058, Rev. 2, Pacific Northwest National Laboratory, Richland, Washington, USA (2012).
14. G. L. HAWKES, "AGR-1 Daily As-run Thermal Analyses," ECAR-968, Rev. 4, Idaho National Laboratory, Idaho Falls, USA (2014).